

# Analysis of Mechanisms of Rock Destruction in Electro Discharge Drilling

Burkin V.V., Kuznetsova N.S., Lopatin V.V

High Voltage Research Institute, Lenina Avenue 2A, Tomsk, 634050, Russia, tel. (3822)423838, fax (3822)418560, tevn@hvd.tpu.ru

**Abstract - Simulation results of electro burst in solid which consistently describes plasma channel expansion, shock waves generation and their interaction with a material is presented. The consecutive solution of wave dynamics equations in condensed material and equations in the discharge circuit of pulse generator has allowed to analyze possible mechanisms of scabbling crater formation in solid. Connection of the discharge circuit parameters with tensely - deformed solid state and destruction character is shown, influence of dielectric surface form and circuit parameters on character of possible destruction is presented. It is showed, that solid destruction occurs due to compression material surrounding the channel and stretching or displacement between the channel and destroyed material surface.**

## 1. Introduction

Material destruction at electrical discharge in electro discharge technologies with laid electrodes, drilling, for example, is determined by discharge power characteristics and physico-mechanical properties of destroyed rock. Depending on discharge energy, speed of wave distribution generated by the expanding plasma channel, depth of channel inculcation different variants of wave dynamics and, accordingly, various mechanisms of material destruction nearby its surface can be realized.

It is considered, that the main factor determining solid destruction at electro burst, is the shock wave, radiated by expanding channel which in the neighborhood of the channel (~2-3 mm) transforms in plastic and further in an extending elastic wave with expressed region of tensile tangential stress [1]. Tensely-deformed material state, formed thus, leads to a fracture pattern with the small crush region of material surrounding the channel and extended area of crack formation, covered with a radial crack network [2].

## 2. Electro burst model

The discharge circuit (fig. 1) which includes the plasma channel as an expanding cylinder with resistance  $R_c(t)$  is considered. When S (fig. 1) is switched on solid breakdown occurs. Capacitor energy is released in the channel and discharge channel expands

intensively, that result to stress wave formation and spread in material surrounding the channel.

The scheme of the electrodes disposition, channel trajectory at the moment of bridging electrode gap by discharge channel and variants of wave interaction with dielectric surface are shown on fig. 2. Depth of channel inculcation in solid at optimum regime usually makes  $h \approx 1/3 l_c$  [2]. The variant b) shows a case in which the head part of wave at its output on the dielectric surface is similar to a triangular profile. In case c) stress  $\sigma$  in a wave is gradually reduced in a wave front direction.

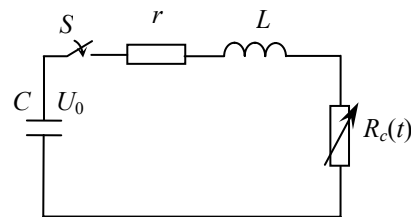


Fig.1. Electrical scheme of the discharge circuit

Electro burst model [3] is based on the laws of pulse, mass, energy preservation describing wave character of pulse influence. The model which consistently describes stored energy transformation  $W_g$  to energy of wave expanding in material, includes the electro-technical equations of circuit, the energy balance equation of plasma channel, the equation of dynamics of tensely - deformed solid state: the movement equation, the indissolubility equation, the energy equation, the equations for tension components, the equations for deformation speed tensor and the granite state equation similar [3].

Simulation was carried out for channel radius  $r_c(0)=5 \mu\text{m}$ ,  $l_c=2 \text{ cm}$ ,  $h=4\dots 8 \text{ mm}$ ,  $C=0.5\dots 20 \text{ nF}$ ,  $U_0=250\dots 350 \text{ kV}$ ,  $L=10\dots 25 \mu\text{H}$ ,  $r_z=1 \text{ Ohm}$ . Numerical integration of the electro-technical equations was carried out by Euler's implicit method. The dynamic equation system [3] was solved consistently and approximated by difference scheme [4] on a computational grid fig. 3, (a). The ordinate axis is an axis of symmetry. In a vicinity of channel calculation cells corresponded to the cylindrical channel form with coordinates of its axis  $x = 0$ ,  $y = 0$ . In vicinity  $y \approx h$  the cells form is adapted to description of wave reflection from a flat surface.

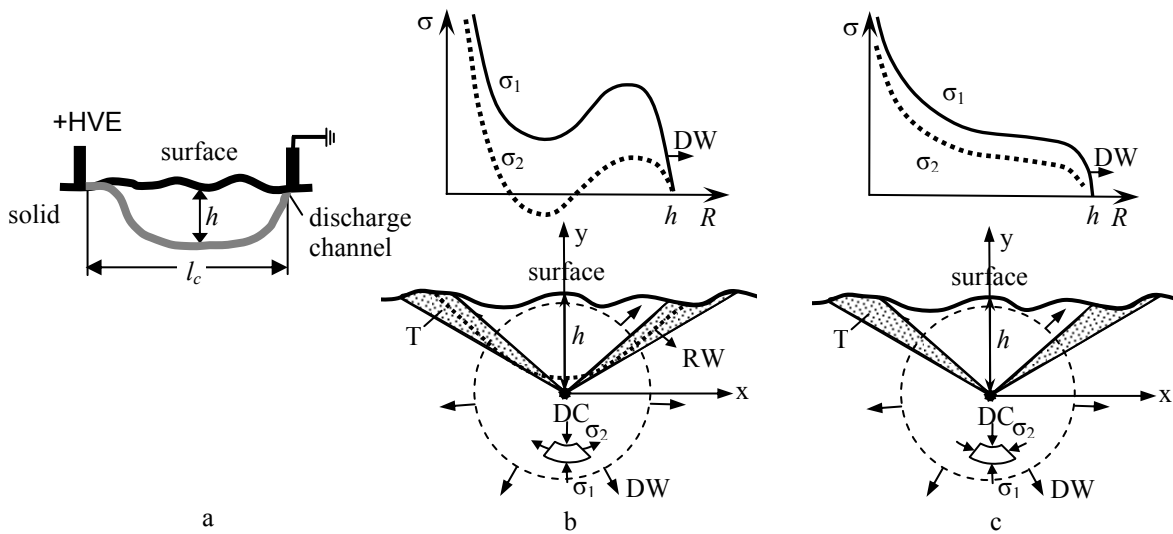


Fig. 2. Scheme of the electrodes disposition and typical channel trajectory (a), sections, perpendicular to the channel (b), (c),  $l_c$  - channel length,  $h$  - depth of channel inculcation, DC - the discharge channel, DW - a direct wave, HVE - a high-voltage electrode, RW - a wave reflected from dielectric surface,  $\sigma_1, \sigma_2$  - radial and tangential stresses, T - areas of the most possible crack formation

Predicted fracture pattern was determined on the basis of analysis of dynamic material tensely - deformed state. In case when distribution of wave stress is similar fig. 2, (b), the main destroying factor is tensile stress arising both in direct and reflected waves. The criterion of destruction  $\sigma = \sigma^*$ , was used to such variant of wave process development, where  $\sigma^*$  is the tensile strength. The material was considered destroyed when one of the stress components has exceeded value  $\sigma^*$ . When the wave

formation is similar fig. 2, (c) wave stresses are compressive in the considered time interval. Destruction in this case is realized when shear deformations exceed critical value. It was necessary, that shear destruction occurs in dielectric regions where shear deformations exceed solid shear strength.

### 3. Simulation results

Typical dependences of stored energy transformation  $W_g$  are shown on fig. 4 where  $W_g = CU_0^2 / 2$ ,

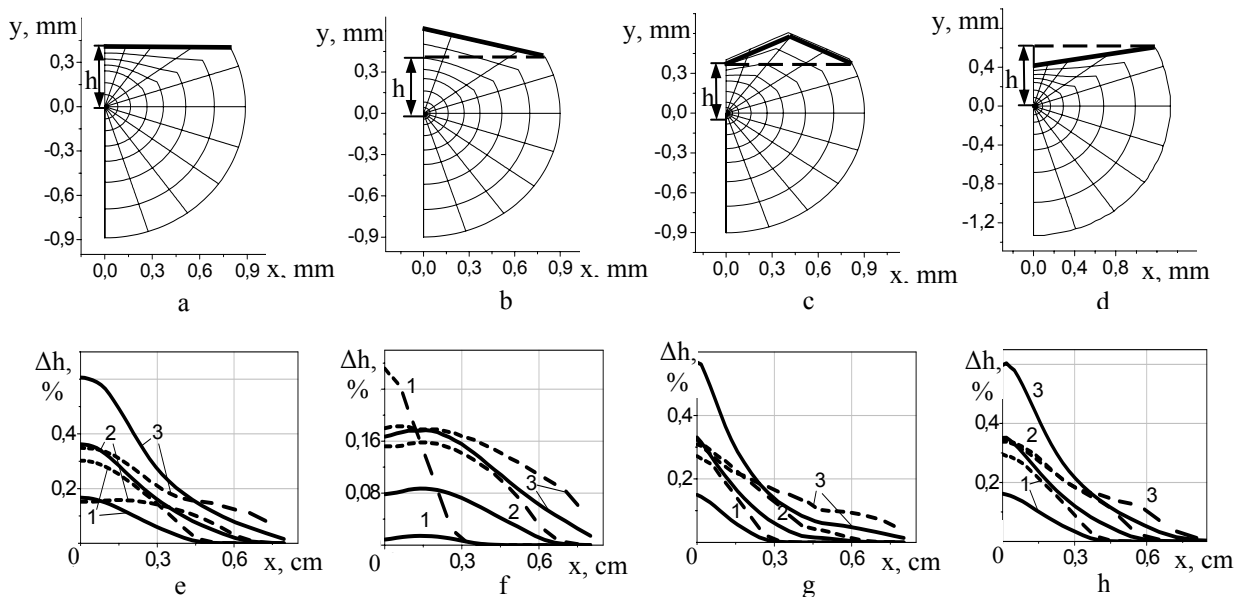


Fig. 3. Surface reflection forms and relative surface displacement  $\Delta h$  of material over the channel:  $U_0=200$  kV, ( )  $C=20$  nF,  $L=25$   $\mu$ H, (----)  $C=0,8$  nF,  $L=1$   $\mu$ H; t,  $\mu$ s: 1 - 1; 2 - 1,25; 3 - 1,5

coefficients of generator energy transformation to the channel  $\eta_c = W/W_g$  and to wave energy  $\eta_w = A/W_g$ , relative power consumption of generating capacity  $\eta_g = CU^2(t)/CU_0^2$ , where  $W$  - channel energy,  $A$  - channel expansion work.

Comparison of time-current dependences and discharge power characteristics fig. 4, (a-b) shows, that only (30÷90) % of storage energy  $W_g$  is used for wave formation to the moment of wave output on a solid surface depending on circuit parameters and channel inculcation depth. Wave energy is still less (5÷25) %  $W_g$ .

Thus the wave profile essentially depends on discharge power parameters. In case fig. 4, (f) tangential stresses become tensile in a direct wave and thereby stimulate radial cracks formation by this stage. In case fig. 4, (c) the tensile stress region in a direct wave has not time to be formed.

The further wave dynamics depends on the solid surface form. Four variants of dielectric surface form were considered in the model fig. 3. Only the right segments of computational grid are resulted due to symmetry. The sizes of surface "roughnesses" did not exceed  $h/2$ . Reaction of material

which is being above the channel on such type of wave influence is showed in moving of a solid part in a surface direction. In sections which divide the moved dielectric part from stationary part, located under a corner  $\alpha$  to Y-line there are displacement deformations. On fig. 5 calculated values of shear deformations  $\varepsilon_{xy}$  in solid elements located in three different sections are showed. Comparison of received distributions  $\varepsilon_{xy}$  shows, that the largest values  $\varepsilon_{xy}$  are in sections located along

$$R = \sqrt{x^2 + y^2} \text{ under corners } \sim 40^\circ \dots 50^\circ \text{ to Y-line.}$$

Dynamics of relative surface displacement  $\Delta h = (h(x,t)/h(x,0) - 1) \cdot 100\%$  for two discharge regimes is shown on fig. 3. It is shown that solid surface raise above the channel is more intensive and decreases to periphery. Comparison of various surface forms shows that only surface on fig. 3 (b) results in qualitative difference of wave dynamics at other forms. With increase in discharge energy  $W_g$  and its duration values  $\Delta h$  also grow. Thus at the identical discharge regimes  $\Delta h$  is the same for different reflection surfaces. It means, that deformation parameters in surface solid layers also are similar in compared cases.

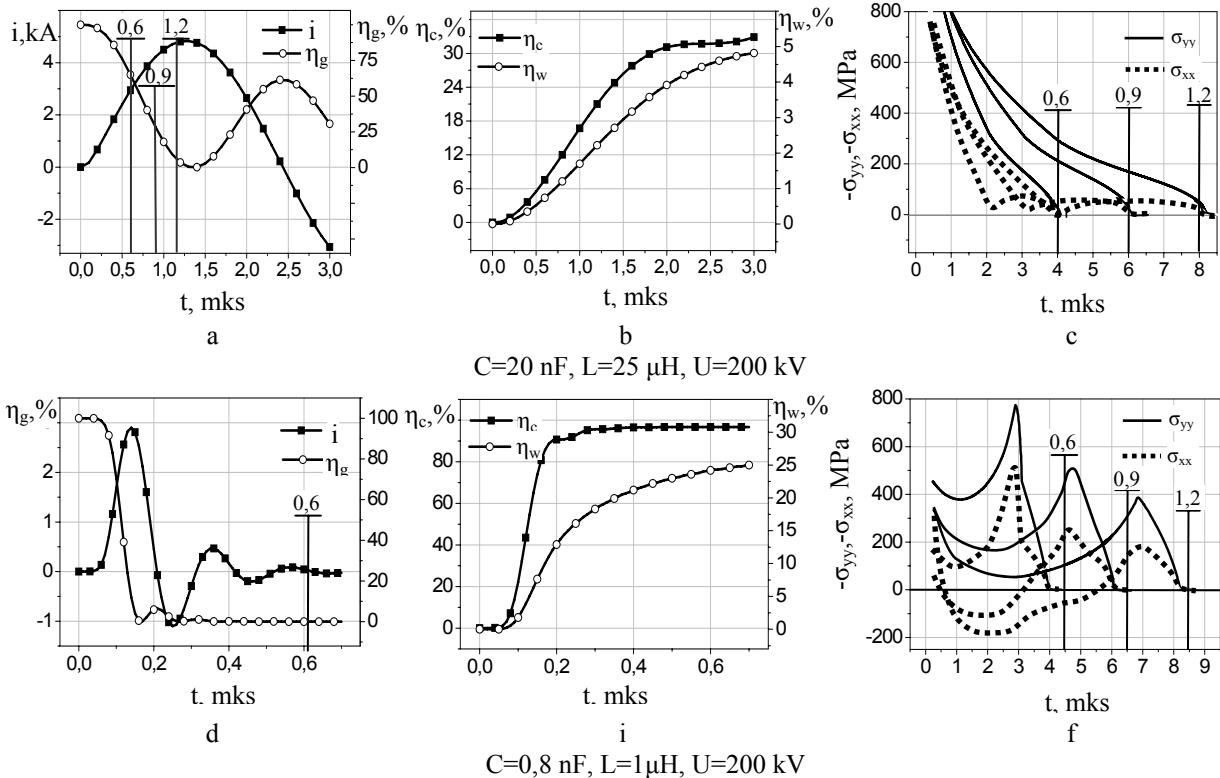


Fig. 4. Time-current dependences  $i$  and energy consumption of generating capacity (a), (d), coefficients of stored energy transformation to the channel energy  $\eta_c$  and to the wave  $\eta_w$  (b), (e), at  $U_0=300$  kV. Stress distribution  $\sigma_{yy}$  (continuous lines),  $\sigma_{xx}$  (lines marked by points) (c), (a) in the wave during the moment of wave output on dielectric surface. The merker  $\Upsilon$  indicates the time 0,6; 0,9; 1,2  $\mu$ s of wave output on a surface located in 4, 6, 8 mm away from the channel, accordingly

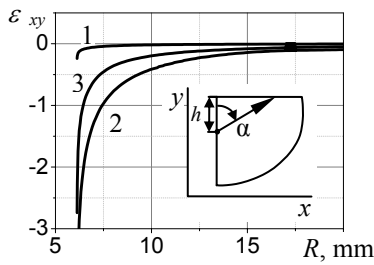


Fig. 5. Dependence of shear deformation on distance  $R$  at  $t=2 \mu\text{s}$ ,  $h=4 \text{ mm}$ ;  $C=20 \text{ nF}$ ,  $L=25\mu\text{H}$ ,  $U_0=200 \text{ kV}$ ,  $\alpha$ : 1)  $0^\circ$ , 2)  $40^\circ$ , 3)  $70^\circ$

Stress distribution in sections located along  $R$  under corners  $40^\circ$ - $50^\circ$  to Y-line (in areas "T" see fig. 2, b, c) are shown on fig. 6

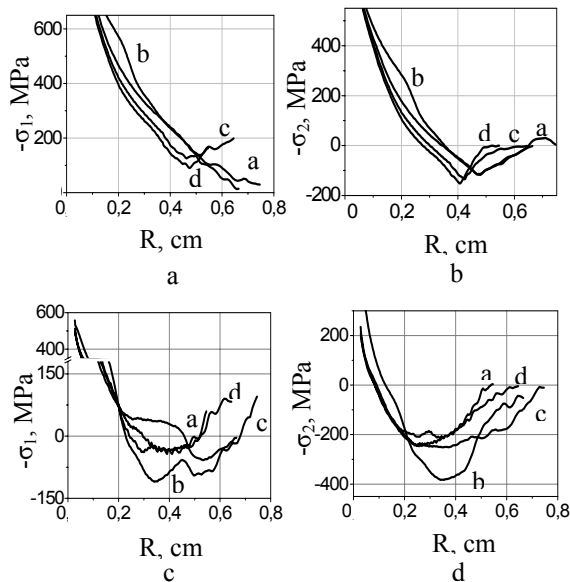


Fig. 6. Main radial  $\sigma_1$  and tangential  $\sigma_2$  stress distribution at  $t=1,5 \mu\text{s}$ ,  $U_0=200 \text{ kV}$  a), b)  $C=20 \text{ nF}$ ,  $L=25 \mu\text{H}$ ; c), d)  $C=0,8 \text{ nF}$ ,  $L=1 \mu\text{H}$ . Letters correspond to reflection surface forms on fig. 3

Comparison of the main radial  $\sigma_1$  and tangential  $\sigma_2$  stresses shows, that high-energy discharge regimes do not result in tensile stress region formation (fig. 6, a, b). Crack formation in region "T" is connected with exceeding by shear deformation of critical values. In these cases the mechanism of scabbling crater formation is realized at large wave energy and practically does not depend on the reflection surface form. Less-energy discharge re-

gimes lead to formation of tensile tangential stress area already in a direct wave which intensifies at reflection fig. 6, d. As a result radial cracks which lead to scabbling crater formation are formed. Tensile tangential stress and sizes of destruction regions are more critical to the reflection surface form as against the previous case. It means, that volume of formed scabbling crater also depends on conditions of wave reflection from a surface. Thus the considered mechanism of scabbling crater formation is considerably less power-expenditure.

At the circuit parameter variation and different value  $h$  it was shown, that the mechanism of shear destruction becomes the main with increase in generator energy  $CU_0^2/2$ , growth of discharge duration and at small channel inculcations.

#### 4. Conclusion

Two possible mechanisms of rock destruction and scabbling crater formation are found by electro burst simulation. More powerful and durable discharge forms scabbling crater due to shear deformations. Coefficient of generator energy transformation to the wave energy makes  $\sim 4 - 5 \%$ , and mechanism of scabbling crater formation practically does not depend on the reflection surface form. Less powerful and less durable discharge forms a scabbling crater due to tensile tangential stress in a wave. The corresponding coefficient of energy transformation has increased up to  $15 \%$  and more. Influence of the reflection surface form on tensely - deformed solid state and, hence, on the cavity sizes occur only in case of destruction due to tensile stress.

#### References

- [1] V.V. Burkin, Physics of burning and explosion, № 4, pp. 113-118.(Russian)
- [2] B.V Semkin., A.F. Usov, N.T. Zinovjev, *Transients in installations of electropulse technology*, Saint Petersburg, Science, 2000, P. 223. (Russian)
- [3] V.V. Burkin, N.S. Kuznetsova, V.V. Lopatin, *Bulletin of TPU*, №2, 2006.
- [4] M.L. Wilkins, *Calculation of elastic - plastic currents. Computing methods in hydrodynamics*. Under edition F. Older, Moscow, Mir, 1967, pp. 212-263.